Structural assembly of the signaling competent ERK2–RSK1 heterodimeric protein kinase complex

Anita Alexa[a,1], Gergő Gógl[a,b,1], Gábor Glatz[a], Ágnes Garai[b], András Zeke[a], János Varga[b], Erika Dudás[c], Norbert Jeszenői[d], Andrea Bodor[c], Csaba Hetényi[e], and Attila Reményi[a,2]

[a]Lendület Protein Interaction Group, Institute of Enzymology, Research Centre for Natural Sciences, and [e]MTA-ELTE Molecular Biophysics Research Group, Hungarian Academy of Sciences, 1117 Budapest, Hungary; Departments of [b]Biochemistry and [d]Genetics, Eötvös Loránd University, 1117 Budapest, Hungary; and [c]Institute of Chemistry, Laboratory of Structural Chemistry and Biology, 1117 Budapest, Hungary

Edited by Robert M. Stroud, University of California, San Francisco, CA, and approved January 27, 2015 (received for review September 12, 2014)

Mitogen-activated protein kinases (MAPKs) bind and activate their downstream kinase substrates, MAPK-activated protein kinases (MAPKAPKs). Notably, extracellular signal regulated kinase 2 (ERK2) phosphorylates ribosomal S6 kinase 1 (RSK1), which promotes cellular growth. Here, we determined the crystal structure of an RSK1 construct in complex with its activator kinase. The structure captures the kinase–kinase complex in a precatalytic state where the activation loop of the downstream kinase (RSK1) faces the enzyme's (ERK2) catalytic site. Molecular dynamics simulation was used to show how this heterodimer could shift into a signaling-competent state. This structural analysis combined with biochemical and cellular studies on MAPK→MAPKAPK signaling showed that the interaction between the MAPK binding linear motif (residing in a disordered kinase domain extension) and the ERK2 "docking" groove plays the major role in making an encounter complex. This interaction holds kinase domains proximal as they "readjust," whereas generic kinase domain surface contacts bring them into a catalytically competent state.

protein kinase | signal transduction | structural biology | ERK2 | RSK1

Protein kinase activity is controlled by phosphorylation at its activation loop by upstream kinases (1, 2). Therefore, a catalytically competent kinase–kinase pair must involve surface contacts around the catalytic center of the upstream kinase binding to the activation loop of the downstream kinase. Because of the transient and presumably highly dynamic nature of these enzyme–substrate interactions, little is known about the structural assembly of cognate kinase–kinase pairs. For example, the pivotal role of mitogen-activated protein kinase (MAPK)→MAPK-activated protein kinase (MAPKAPK) signaling events propagating mitogenic and stress signals is well established, but it is structurally not known how a catalytically competent MAPK–MAPKAPK enzyme–substrate complex forms.

Extracellular signals or mitogen stimulation activate the extracellular signal regulated kinase (ERK) pathway, which comprises a hierarchically organized kinase cascade (3, 4). ERK2 becomes phosphorylated by upstream MKK1/2 kinases on a threonine (Thr185) and a tyrosine (Tyr187) residue located in its activation loop (5). In turn, activated ERK1/2 activates ribosomal S6 kinase 1 (RSK1) by sequential phosphorylation events where double-phosphorylated ERK1/2 (ppERK1/2) first phosphorylates the C-terminal RSK1 kinase domain at its activation loop (on Thr573). This is required for the activation of the N-terminal AGC kinase-type domain that will in turn become capable of phosphorylating cell growth promoting substrates (6). Other MAPKAPKs such as MAPKAPK2 (MK2) or MAP kinase-interacting serine/threonine-protein kinase 1 (MNK1) have only one kinase domain that directly phosphorylates downstream substrates. The three proteins are evolutionarily related, activated by MAPKs similarly, but they play markedly different physiological roles (7).

In addition to the transient interactions forming between enzyme–substrate kinase domain pairs, efficient phosphorylation of all 11 mammalian MAPKAPKs by MAPKs (e.g., ERK1/2 and p38 kinases) requires an intact ∼20- to 30-amino-acid-long extension following the C-terminal kinase domain (8–10). This region harbors a MAPK binding consensus sequence referred to as a linear motif (LM) (11). MAPKAPKs all contain a domain related to the kinase domain of calcium/calmodulin-dependent kinases (CAMKs), which is phosphorylated in its activation loop by activated MAPKs. This is the first step in MAPKAPK activation (12, 13). Different MAPKAPKs have diverse sets of substrates but the first step of MAPK→MAPKAPK activation may share a common mechanism.

In the present study, we determined the crystal structure of unphosphorylated ERK2 in complex with an RSK1 construct composed of the C-terminal kinase domain and the linear motif (hereafter referred to as RSK1). The complex is in a precatalytic quaternary arrangement where the activation loop of the downstream kinase (RSK1) faces the enzyme's (ERK2) catalytic site.

Results

Crystal Structure of ERK2–RSK1 Captures a MAPK–MAPKAPK Complex in a Precatalytic State. To structurally elucidate protein–protein interactions involved in the first step of RSK1 activation, we determined the crystal structure of unphosphorylated ERK2 bound to RSK1 at 2.15-Å resolution (R_{free} = 20.8%; *SI Appendix*, Table S1). This complex captured the quaternary structure of

Significance

Signaling pathways often use kinase cascades, but structural characterization of catalytic complexes between heterodimeric kinase pairs has been elusive. For MAPK–MAPKAPK binary complexes, a high-affinity "docking" interaction holds kinase domains proximal within a tethered complex. This heterodimer provided a unique opportunity to shed light on kinase domain–domain contacts that play a role in the assembly of the transient catalytic complex. Starting out from a new precatalytic extracellular signal regulated kinase 2–ribosomal S6 kinase 1 (ERK2–RSK1) crystallographic complex, where the activation loop of the downstream kinase (RSK1) faced the enzyme's (ERK2) catalytic site, we used molecular dynamics simulation to show how the catalytic ERK2–RSK1 complex forms. Our findings reveal the dynamic process through which transient, physiologically relevant kinase heterodimers form in a prototypical kinase cascade.

Author contributions: A.A., G. Gógl, and A.R. designed research; A.A., G. Gógl, G. Glatz, Á.G., A.Z., J.V., E.D., and C.H. performed research; A.A., G. Gógl, G. Glatz, Á.G., A.Z., E.D., N.J., A.B., C.H., and A.R. analyzed data; and A.R. wrote the paper.

The authors declare no conflict of interest.

This article is a PNAS Direct Submission.

Freely available online through the PNAS open access option.

Data deposition: The atomic coordinates and structure factors have been deposited in the Protein Data Bank, www.pdb.org (PDB ID code 4NIF).

[1]A.A. and G. Gógl contributed equally to this work.

[2]To whom correspondence should be addressed. Email: remenyi.attila@ttk.mta.hu.

This article contains supporting information online at www.pnas.org/lookup/suppl/doi:10.1073/pnas.1417571112/-/DCSupplemental.

a MAPK–kinase substrate pair in which the activation loop of the downstream kinase is positioned next to the catalytic site of its activator kinase (Fig. 1*A*). The face-to-face stoichiometric complex displays a bipartite protein–protein interface with a buried surface area of ~1,500 Å^2. The RSK1 linear motif region forms several hydrogen bonds, salt bridges, and side-chain–specific van der Waals interactions in the MAPK docking groove (interface 1, IF1) (Fig. 1*B*). This part of the new protein–protein complex shows an excellent agreement to the crystal structure of ERK2 bound to the chemically synthesized RSK1 linear motif peptide (11). The second interface (interface 2, IF2) forms between the two kinase domains and it makes up half of the total interaction surface. IF2 is dominated by van der Waals interactions and it forms between generic kinase features that are highly conserved across different kinase families (e.g., Ala-Pro-Glu, APE motif, the conserved segment of the kinase activation loop or the P loop involved in ATP cofactor binding) (Fig. 1*B*). In contrast, IF1 involves the so-called MAPK docking groove, which is a protein surface that shows topographical diversity even between closely related MAPK family members (e.g., ERK2, p38α) (11).

To test whether the observed face-to-face arrangement of the complex plays a role in RSK1 activation, we analyzed the impact of binding surface disrupting mutations: (*i*) RSK1 was mutated in a central linear motif position (the leucine in φ_A was changed to glutamate, L714E) or (*ii*) the linker connecting the linear motif and the kinase domain was shortened by 2, 4, and 6 residues (RSK1_ΔL2,4,6). RSK1 activation by preactivated ERK2 was monitored in in vitro kinase assays (Fig. 2*A*). Whereas phosphorylation of RSK1_ΔL2 and RSK1_ΔL4 was only slightly affected, the initial rate of Thr573 phosphorylation was greatly decreased with RSK1(L714E) and RSK1_ΔL6 compared with the wild-type substrate (*SI Appendix*, Fig. S1*A*). Differences were not due to impaired structural integrity of RSK1 constructs as mutants and wild-type displayed identical circular dichroism spectra (*SI Appendix*, Fig. S1*B*). The reduced rate of RSK1(714E) activation is likely due to its impaired capacity to bind to ERK2 as their binding affinity is greatly reduced (>50 μM) (*SI Appendix*, Fig. S1*C*). In contrast, RSK1_ΔL6 binds ERK2 with similar affinity compared with wild type (K_d ~ 0.2 μM), but it is a suboptimal substrate because its reduced linker length presumably limits formation of contacts in the face-to-face ERK2–RSK1 heterodimer at IF2.

Next, phosphorylation of RSK1 mutants was examined in a cell-based assay to examine the physiological relevance of the crystallographic complex. HEK293 cells were transiently transfected with RSK1 mutant constructs or with wild type, the ERK pathway was stimulated by addition of epidermal growth factor (EGF), and RSK1 phosphorylation following endogenous ERK2 activation was monitored by Western blots using a phospho-RSK1(Thr573) antibody (Fig. 2*B*). This cell-based assay showed that RSK1(L714E) and the RSK1_ΔL6 both had reduced phosphorylation compared with wild type. Blocking ERK–RSK1 interaction through IF1 appeared to have a more severe impact in cells [RSK1(L714E)]; nevertheless, EGF stimulation also caused diminished RSK1_ΔL6 activation. In summary, these experiments suggest that, despite the fact that ERK2 was unphosphorylated in the complex, the ERK2–RSK1 crystal structure captured a physiologically relevant heterodimeric state that plays a role in ERK2→RSK1 activation.

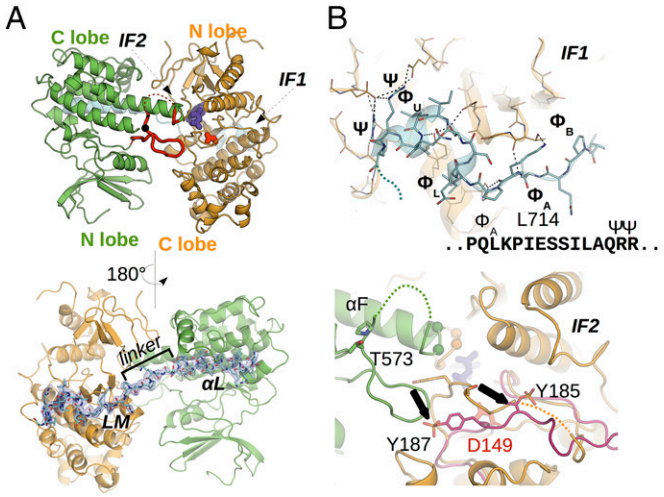

Fig. 1. Structure of the ERK2–RSK1 complex. (*A*) Crystal structure of the ERK2 (orange)–RSK1 (green) complex. The RSK1 linear motif region binds to the MAPK docking groove (interface 1, IF1). RSK1 forms a face-to-face antiparallel kinase dimer with the ERK2 kinase domain through IF2 where the catalytic aspartate (Asp149, shown in red) is located next to the RSK1 activation loop (shown in red, and Thr573 is shown with a black sphere). The nucleotide cofactor (AMPPNP) is colored blue. The unstructured part of the RSK1 loop is shown with a dashed line. *Lower* shows the complex from the back where the electron density for the linear motif (LM), αL, and the intervening linker region (colored in cyan) is shown with sigmaA-weighted omit map contoured at 1σ. (*B*) A close view of IF1 and IF2. At IF1, contacts are highlighted and labeled according to linear motif consensus (11). Black dashed lines indicate H-bond interactions. At IF2 contacts form between the APE motif of RSK1 and the P loop of ERK2 (Cα atoms of residues within van der Waals contacts are shown with spheres). The dephosphorylated activation loop of ERK2 blocks the RSK1 phosphorylation site (Thr573 in the TP motif) from accessing the ERK2 active site (Asp149, shown in stick representation in red) and substrate binding pocket. The ppERK2–RSK1 complex was generated by superposing the ppERK2 structure (PDB ID: 2ERK) with ERK2 from the crystallographic complex. The phosphorylated activation loop of ERK2 (with Tyr187 and Thr185) is shown in purple.

Molecular Dynamics on ERK2–RSK1 Complexes. The ERK2 catalytic center and the RSK1 activation loop face each other in the unphosphorylated ERK2–RSK1 complex. The enzyme's active site (Asp149), however, is shielded off from the substrate by the unphosphorylated ERK2 activation loop (Fig. 1*B*). Thus, this crystallographic model likely captures the snapshot of a precatalytic MAPK–MAPKAPK complex. In contrast, to inactive ERK2, the activated form has an open active site (5) (Fig. 1*B*). Therefore, we used the ERK2–RSK1 binary complex crystal structure as the basis for generating a phosphoERK2–RSK1 model by superpositioning double phosphorylated ERK2 (ppERK2) with unphosphorylated ERK2 within this complex. The complexes were then subjected to molecular dynamics (MD) simulations.

Unrestrained MD simulation on ppERK2–RSK1 showed markedly different movements of the activator and substrate kinase domains relative to each other compared with the complex containing unphosphorylated ERK2. Principal component analysis of MD results revealed great differences: Diverse domain orientation movements suggested a conformationally divergent ERK2–RSK1 complex, whereas intramolecular movements were dominating in the ppERK2–RSK1 complex. These latter appeared to maximize/optimize the interaction surface around ERK2's catalytic core (*SI Appendix* and Movie S1). During these simulations IF1 was highly stable, displaying only small range variations. In contrast, kinase domain–domain contacts (around IF2) changed greatly and the buried surface area increased compared with the starting state (*SI Appendix*, Fig. S2*A*). The interaction between the APE motif of RSK1 and the P loop from ERK2 was stable for both complexes during the 150-ns-long MD run, and this prominent contact surface appeared as a pivot point around which the kinases swiveled to optimize their interaction surface (*SI Appendix* and Movies S2 and S3). Although the interaction surface increased for both complexes, indicating that this can be optimized compared with what was observed in the crystallographic complex, contacts became more extensive in the ppERK2–RSK1 complex. This was because RSK1 formed a unique surface with ppERK2 in addition to contacts formed with unphosphorylated ERK2. Unique contacts formed between residues of αD and αG

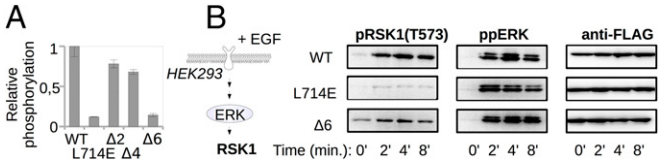

Fig. 2. Experimental validation of ERK2–RSK1 contacts. (*A*) RSK1 mutants display reduced phosphorylation by preactivated ERK2. Phosphorylation rate of RSK1 was monitored by in vitro kinase assays (*SI Appendix*, Fig. S1). L714E has a mutation at IF1, whereas linker length mutants (Δ2–6) affect contacts at IF2 indirectly. The bar graph shows relative RSK1 phosphorylation, which was calculated based on initial phosphorylation rates that were normalized to wild type (WT), and error bars show the SDs from mean value; $n = 3$ experiments (*SI Appendix*, Fig. S1*A*). (*B*) RSK1 mutants display reduced activation capacity upon EGF stimulation in HEK293 cells. (*Right*) Representative set of three independent experiments where samples were taken at the indicated time points after EGF treatment of serum-starved HEK293 cells. Heterologous RSK1 and endogenous ERK activation, the latter as a control for EGF treatment, were monitored by Western blots with phospho-RSK1 (Thr573) and ppERK2-specific antibodies, respectively. Transiently transfected RSK1 constructs had a FLAG tag, and anti-FLAG Western blotting was used to demonstrate equal load for different samples and uniform transfection efficiency for different experiments.

from the C lobe of ppERK2 and the N lobe of RSK1 (e.g., residues from the P loop, and from loops connecting β3 and αC or β4 and β5) (*SI Appendix*, Fig. S2*B*).

Next, we validated the importance of contacts suggested by the ppERK2–RSK1 MD model. Ser452 and Glu623 are located on the N- and C-terminal RSK1 kinase lobes, on the β3–αC loop and on αG, respectively (Fig. 3*A*). Note that Ser452 and Glu623 are located on contact surface patches that were implicated by MD simulations only and they do not form contacts within the ERK2–RSK1 crystal structure (*SI Appendix*, Fig. S3*A*). These two residues were mutated to bulky tryptophan amino acids. MD indicated that the RSK1 APE motif is at the center of kinase domain contacts in the ERK2–RSK1 heterodimer and this region was also subjected to amino acid replacements. The impact of these mutations or their combination were tested in in vitro kinase assays and in cell-based assays (Fig. 3 *B* and *C* and *SI Appendix*, Fig. S3 *B* and *C*). In line with the results of in vitro kinase assays, RSK1 mutants got activated less in a cell-based assay where ERK2 and RSK1 phosphorylation was triggered by stimulating cells with EGF. To demonstrate that RSK1 mutants were structurally intact and could bind ERK2 through their linear motif region, the RSK1(APE/623) construct was subjected to circular dichroism and ERK2 binding measurements (*SI Appendix*, Fig. S3*D*). This RSK1 mutant, that ppERK2 activated the least, did not show any difference compared with wild type, indicating that its structure and enzyme binding capacity stayed intact. Because amino acid replacements had to be made on an extensive, presumably dynamic and "loose" interface where van der Waals interactions appeared to dominate, residues were changed to bulky amino acids such as to tryptophan or arginine instead of alanines. We argued that some local clashes would rather impede dynamic complex assembly as opposed to mere side-chain shortening on an extensive IF2-like surface. In summary, our experimental results validated ERK2–RSK1 MD models and show that we correctly identified kinase domain contacts that govern signaling in a physiologically relevant catalytic complex.

Structural Model of the Catalytic ppERK2–RSK1 Complex. The ppERK2–RSK1 MD model clearly demonstrated that the critical RSK1 activation loop region containing Thr573 and Pro574 could flip into the ERK2 substrate binding pocket without perturbing the compact quaternary arrangement observed in the 150-ns-long MD simulation (Fig. 4). Because this structural model was conducive to a signaling competent complex, we attempted to obtain a structural model for a catalytic ppERK2–RSK1 enzyme–substrate complex. The catalytic aspartate (Asp149) is ~30 Å apart from Thr573 of RSK1 in the ERK2–RSK1 crystal structure (measured between their Cα atoms), but MD simulations indicated that the RSK1 activation loop is a highly flexible region of the kinase domain (*SI Appendix*, Fig. S4*A*). The distance between Thr573 (RSK1) and Asp149 (ERK2) indeed decreased in the course of the 1-μs-long unrestrained MD simulation on ppERK2–RSK1 (*SI Appendix*, Fig. S4*B*). However, the simulation time was presumably not long enough to capture the catalytic complex where the RSK1 TP motif binds into the ERK2 substrate pocket and becomes optimally positioned for phosphotransfer. Similarly to other so-called proline-directed serine–threonine kinases, the substrate binding pocket of MAPKs accepts serine or threonine residues that are followed by a proline (S/TP motifs). Because proline-directed kinases presumably bind their substrates similarly, an optimal distance for the two critical ERK2 and RSK1 residues could be obtained based on a related proline-directed kinase–substrate complex structure (14). The Thr-Pro motif region of the RSK1 activation loop was superimposed with the corresponding residues from the DYRK1A–substrate peptide complex and the loop conformation was minimized (*SI Appendix*, Fig. S4*B*). This approach gave a feasible "restrained" structural model for the catalytic ppERK2–RSK1 complex. Moreover, energy calculations on the starting, the unrestrained, and the restrained models indeed indicated that the catalytic interface increasingly contributed to the total computed interaction energy of the ppERK2–RSK1 complex (*SI Appendix*, Fig. S4*C*).

Role of the MAPKAPK APE Motif in Activator Kinase Binding. The major contact between kinases at IF2 forms between the glycine-rich P loop of ERK2 and the APE motif of RSK1 in the ERK2–RSK1 crystal structure. In addition, MD simulations on ppERK2–RSK1 implicated these generic regions as pivots around which kinase domain contacts get optimized during ppERK2→RSK1 phosphorylation. In kinases the P loop is involved in ATP binding and ADP release, whereas the APE motif plays a pivotal role in protein substrate binding at the P+ side (15). In calcium/calmodulin-dependent protein kinases (CAMKs) an inhibitory helix sterically blocks the binding of substrates by occluding the substrate binding pocket (16). Similarly, the αL helix plays the same role in the related C-terminal kinase domain of MAPKAPKs (Fig. 5*A*). In contrast to other known protein kinases, the APE motif occupies a noncanonical position in all inactive MAPKAPK structures (for example it is part of the extended αF helix in known RSK structures), whereas in their active state—after

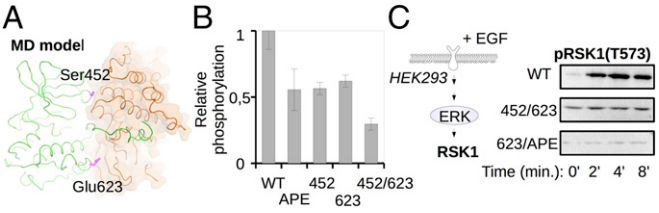

Fig. 3. Experimental validation of surface contacts from the ppERK2–RSK1 MD model. (*A*) MD predicts that Ser452 and Glu623 play a role in the catalytic ppERK2–RSK1 complex. Phosphorylation rate of RSK1 was monitored by using in vitro kinase assays (*SI Appendix*, Fig. S3*B*). (*B*) The bar graph shows relative RSK1 phosphorylation, which was calculated based on initial phosphorylation rates that were normalized to wild type (WT), and error bars show the SDs from mean value; $n = 3$ experiments. (APE: RSK1 mutant with a modified APE motif; 452 or 623: Ser452 or Glu623 were changed to tryptophans; APE/623: two mutated regions are combined within one RSK1 construct.) (*C*) Results of RSK1 activation in EGF-stimulated cells. Blots show a representative set of three independent experiments where samples were taken at the indicated time points after EGF treatment of serum-starved HEK293 cells. Heterologous RSK1 and endogenous ERK activation or equal protein load were analyzed similarly as in Fig. 2 (and control blots for ppERK and RSK1 level are shown on *SI Appendix*, Fig. S3*C*). (For comparison, the blot for WT is the same as in Fig. 2.)

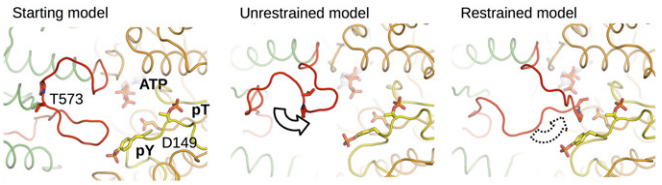

Fig. 4. MD simulations on the ppERK2–RSK1 complex. Movements of the RSK1 activation loop are highlighted (in red). "Starting model" shows a close-up around the catalytic center; the "unrestrained" model shows the same region from the MD model that displayed the shortest distance between Thr573(RSK1) and Asp149(ERK2) (*SI Appendix*, Fig. S4*B*); and the "restrained model" was generated by modeling the RSK1 activation loop based on the DYRK1A–substrate peptide complex (14) (*SI Appendix*, Fig. S4*B*).

MAPK-mediated phosphorylation on their activation loop—this region presumably displaces αL so as to play the same pivotal role in substrate binding as in all kinases (Fig. 5*B*) (17).

The APE motif region of αF may undergo a major conformational change that is triggered by phosphorylation of the MAPKAPK activation loop. These intramolecular rearrangements then create a functional substrate binding pocket on MAPKAPKs (17, 18). For RSK1, and presumably for other MAPKAPKs, the APE region is also involved in activator kinase binding in addition to its canonical role in downstream substrate binding. Thus, uniquely, the MAPKAPK APE region plays a dual role. The ERK2 P loop in the complex also has an unexpected role: In addition to ATP binding, it is involved in substrate kinase binding as it contacts the RSK1 APE motif (Fig. 1*B*).

Determinants of MAPK→MAPKAPK Signaling Specificity. Bimolecular fluorescence complementation (BiFC)-based cellular assays showed that the RSK1 linear motif is absolutely necessary to mediate the binary interaction between ERK2 and its substrate kinase in the cell (*SI Appendix*, Fig. S5). In addition, we formerly showed that linear motif containing peptides from RSK1, MK2, and MNK1 bind to MAPKs with well-defined selectivity profiles that match to MAPK→MAPKAPK biological specificity: RSK1 and MK2 linear motif peptides bound their cognate MAPKs with submicromolar affinities (<0.5 μM), whereas they bound noncognate MAPKs weaker (K_d ~ 10–20 μM) (11). In agreement with the biological role of MNK1, the linear motif containing peptide from this protein bound both to ERK2 and p38α with equal (~0.5 μM) binding affinity (11). Here, we examined the behavior of three MAPKAPK peptides in solution using NMR-based secondary chemical shift (SCS) analysis (*SI Appendix*, Fig. S6). Variation of SCS values for Hα, Cα, and Cβ resonances along the peptide chain can reveal secondary structure propensities in unfolded and partly folded proteins. Although all linear motif peptides adopt a characteristic binding conformation upon binding to MAPKs, they were found to be disordered in solution. This analysis in combination with structure solution of MAPKs in complex with linear motif containing peptides and MAPK–MAPKAPK protein–protein complexes suggests that these MAPKAPK regions undergo disorder-to-order transition upon binding to the MAPK "docking" groove (11, 19). This is also supported by the fact that these regions are disordered in monomeric crystal structures of RSK2 and MK2 (17, 20).

RSK1 and MK2 MAPKAPKs are specifically activated by ERK2 and p38 MAPKs, respectively, whereas MNK1 is activated by both MAPKs in cells. To address how distinct interfaces contribute to MAPK–MAPKAPK signaling, we monitored MAPK→MAPKAPK phosphorylation by in vitro kinase assays using purified proteins (*SI Appendix*, Figs. S7 and S8). Changing the unspecific linear motif in MNK1 into a MAPK specific motif (pepRSK1 or pepMK2) mildly shifted chimera construct phosphorylation toward corresponding MAPKs as expected (*SI Appendix*, Fig. S8 *A* and *B*). Similarly, phosphorylation of RSK1 and MK2 chimera constructs showed agreement to the MAPK binding specificity profile of their linear motif region (*SI Appendix*, Fig. S8 *C* and *D*). However, RSK1 and MK2 were phosphorylated not only by their cognate MAPKs but also by noncognate MAPKs (10). Particularly, ERK2-mediated phosphorylation of MK2 was unexpectedly high, close to half of what was observed on RSK1 (*SI Appendix*, Fig. S8*C*). Mitogen stimulus involving ERK2 leads to RSK1 but not to MK2 activation in the cell (10, 13), although MK2 was first identified as an in vitro ERK2 substrate (21), biochemical specificity of binary MAPK→MAPKAPK pairs is clearly not sufficient to explain physiological specificity. In the cell, however, MAPKs work in the context of other MAPKs. Thus, inactive p38α may efficiently hinder signaling through the ERK2–MK2 noncognate kinase pair indirectly. The mechanism is based on interfering with noncognate recruitment of ERK2 to MK2 because inactive p38α can bind to the MK2 linear motif region with higher affinity compared with activated ERK2. When similar in vitro kinase assays were carried out in the presence of inactive p38α, ERK2-mediated phosphorylation of MAPKAPKs indeed became specific and "leakage" between noncognate pairs was abolished (*SI Appendix*, Fig. S8*E*).

These results suggest that linear motif regions have a pivotal initiator role in complex formation, possibly by tethering the two kinase domains next to each other. Once an activated MAPK is recruited, MAPKAPK activation loop phosphorylation progresses in a nonselective fashion. Correct physiological specificity was achieved only in the presence of noncognate MAPKs when illicit MAPK recruitment was efficiently blocked. Thus, additional surfaces on kinase domains do not greatly influence signaling specificity. Leakage, however, is influenced by MAPKs from other signaling pathways, suggesting that higher level contextual factors also contribute to correct MAPK→MAPKAPK signaling in the cell (*SI Appendix*, Fig. S8*F*).

Discussion

Structural and biochemical characterization of MAPK–MAPKAPK complexes suggest the first mechanistic model on the structural assembly of a signaling competent kinase heterodimer (Fig. 6). This model explains the pivotal role of the linear motif region in MAPKAPKs and it highlights the role of various catalytic and noncatalytic kinase surfaces. The short MAPKAPK linear motif region likely promotes the assembly of an encounter complex in which the kinase domains are randomly oriented. This complex is tethered together through a linear motif mediated interaction

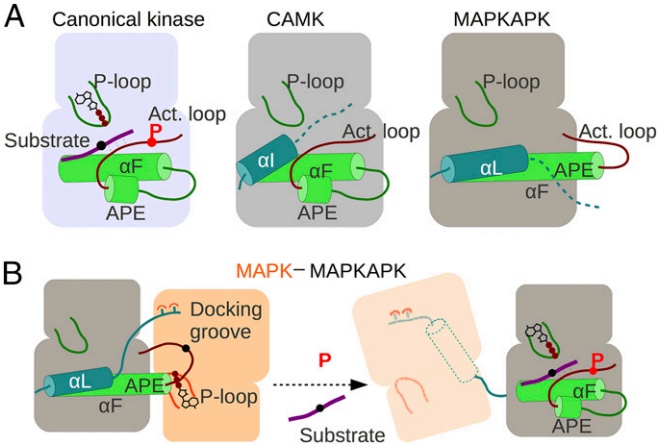

Fig. 5. Role of the MAPKAPK APE motif and the MAPK P loop in substrate or activator kinase binding. (*A*) Inactive, unphosphorylated MAPKAPKs have a unique APE motif region different from related Ca^{2+}/calmodulin-dependent protein kinases (CAMK) or from a canonical kinase. (*B*) Schematic model of a MAPK→MAPKAPK(CTD) signaling complex. The model depicts the dual role of the APE motif in activator kinase binding for unphosphorylated MAPKAPKs as well as in downstream substrate binding after MAPKAPK activation loop phosphorylation.

engaging the MAPK docking groove (IF1). The "encounter complex" provides the possibility of readjustments of kinase domain orientations for maximizing their contacts around IF2 without disassembly ("readjusting complex"). Complete alignment of kinase domains in which the substrate kinase's activation loop binds next to the upstream kinase's catalytic site requires that the MAPK activation loop is double phosphorylated. A precatalytic complex can only transition into a "signaling complex" (modeled by MD in this study) if the MAPK had been activated by upstream kinases formerly. As MAPK activation also involves the MAPK docking groove where MAPK kinases bind to MAPKs, ERK2 activation and RSK1 phosphorylation happens independently in distinct heterodimeric complexes. Acknowledgedly, the crystallographic ERK2–RSK1 complex is not on the pathway to the Michaelis complex, and it likely represents a complex that is unproductive in terms of RSK1 activation as the productive complex has to contain preactivated ERK2. Despite all this, the new ERK2–RSK1 complex was a good starting point for MD to model the ppERK2–ERK2 signaling competent (or Michaelis) complex. Although MAPK cascades are organized by scaffolding proteins that may align and assemble complexes (22), here we demonstrated that interactions between a linear motif and a dedicated docking groove is sufficient to promote the assembly of the catalytic ERK2→RSK1 binary complex. Interestingly, a similar proximity-induced catalytic mechanism was formerly suggested to facilitate efficient phosphorylation of the ERK2 target site in the Ets-1 transcription factor (23, 24).

The MAPK docking groove mediated interface engages the MAPKAPK linear motif. Despite the fact that this interaction does not involve direct contacts relevant for the catalytic enzyme–substrate complex, it is absolutely necessary for MAPK–MAPKAPK complex formation and signaling. Its pivotal role may be explained by at least two independent mechanisms: (*i*) Kinetically, a disordered interacting region may greatly increase the chance of forming an energetically favorable encounter complex because the interaction forms through induced fit. Thus, complex forming collisions require far less precise orientation of the interacting molecules at the first encounter (25, 26). The disorder-to-order transition at the MAPKAPK linear motif likely has only a small entropic cost so as to form a high-affinity encounter complex with its compact MAPK partner. (*ii*) Tethering of kinase domains via a spatially distinct interface may allow readjustments between kinase domains without dissociation of the first MAPK–MAPKAPK encounter complex. Fine tuning involves generic kinase domain regions that will then lead to a signaling competent complex; however, these generic contacts are insufficient without additional specific contacts to drive the formation of a signaling binary complex (*SI Appendix*, Fig. S5). This presumes that kinase–kinase domain orientations can vary in readjusting MAPK–MAPKAPK complexes. This is indeed supported by unrestrained MD simulations on the ERK2–RSK1 complex. In addition, a p38α–MK2 crystallographic model captured an unrelated, noncatalytic quaternary arrangement compared with what is described in this study (*SI Appendix*, Fig. S9) (19, 27). Direct comparison of available MAPK–MAPKAPK crystal structures shows that the ERK2–RSK1 complex is the first structure to our knowledge in which the activation loop of the MAPKAPK is in the vicinity of the MAPK active site. The p38α–MK2 structure captures an unproductive heterodimer as critical enzyme and substrate regions cannot meet as captured in this crystallographic complex. Moreover, this complex showed that the role of the catalytically incompetent complex is the stabilization of unphosphorylated p38. These are in contrast to the ERK2–RSK1 crystallographic complex.

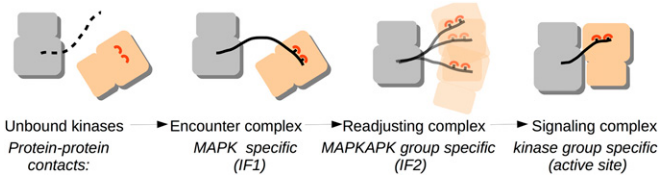

Fig. 6. Model on the structural assembly of the signaling competent MAPK–MAPKAPK complex. The signaling competent ppERK2–RSK1 complex forms through hierarchical assembly of unique, group specific, and common kinase surface contacts. (This scheme is partly speculative but it is consistent with biochemical and structural data presented in this study.)

Interaction at IF1 are highly MAPK specific, as linear motifs have their own characteristic MAPK binding specificity. Formation of contacts at IF2 are likely to be MAPKAPK group specific, as their APE motif is distinct compared with other known kinases, and it has a unique role in upstream kinase binding. MAPKAPK contacts at IF2, however, are less specific within family members as noncognate MAPK–MAPKAPK pairs formed productive complexes if their kinase domains were tethered close artificially (*SI Appendix*, Fig. S8). Overall, contacts through IF1 and IF2 collectively hold the kinase heterodimer in a precatalytic state and the topography of the active site is presumably similar in all proline-directed kinases as these phosphorylate similar target motifs.

Most of our knowledge on kinase dimerization and activation is based on crystal structures of symmetrical homodimers (28). Based on these structures, activation segment exchange for example was suggested to be a common mechanism of kinase autophosphorylation for a subset of protein kinases (29). Dimeric contacts usually form between αG helices, which are normally involved in canonical substrate binding (30–32). Interestingly, this dimerization mode is also observed in known head-to-head heterodimeric complex structures (33, 34). However, the ERK2–RSK1 complex structure revealed an unusual head-to-tail kinase dimerization mode (28). It also revealed alternative functions of well-characterized generic kinase regions, in particular for the P loop and for the APE motif. In addition to the canonical role of the APE motif in substrate binding at the P+ side, its involvement in other protein–protein interactions—such as in upstream activator kinase binding—is unique to MAPKAPKs. This is due to the special position and/or the flexible nature of this motif in inactive MAPKAPKs compared with canonical kinases. Previous structural studies showed that the P loop can directly participate in kinase dimerization. Examples include unrelated, catalytically competent homodimeric structures of the prokaryotic kinase PknB (from *Mycobacterium tuberculosis*) and human checkpoint kinase 2 (CHK2) or the heterodimeric structure of RIP3 and MLKL (31, 34, 35) (*SI Appendix*, Fig. S10). Because the P loop is directly involved in ATP binding by coordinating the β- and γ-phosphate groups for optimal phosphotransfer in all kinases, it may also be that this glycine-rich loop is an ancient allosteric hotspot in precatalytic kinase–kinase complexes.

In conclusion, MAPK→MAPKAPK signaling provides a great example of how generic kinase domain regions could combine with more divergent surface regions in a hierarchical assembly process. This synergism could be particularly important to achieve functional diversity within kinase cascades using similarly built and evolutionarily related enzymatic components. Interestingly, MAPK activation by MAPK kinases (MAPKK), which are also all evolutionarily related, depends on their linear binding motif regions as well (36). Thus, regarding the nature of interactions leading to the formation of a signaling competent kinase–kinase complex, MAPKK→MAPK and MAPK→MAPKAPK activation may be mechanistically alike.

Methods

Protein Production for Structural Studies. The cDNA of full-length human ERK2 and the RSK1 [C-terminal kinase domain (CTD)-LM] construct containing the C-terminal RSK1 region between residues 411 and 735 were cloned into modified pET expression vectors. All protein constructs were expressed in *Escherichia coli* Rosetta (DE3) pLysS (Novagen) cells with standard techniques. Dephosphorylated ERK2 with N-terminal cleavable hexahistidine tag was coexpressed with GST-tagged λ-phage phosphatase. RSK1(CTD-LM) was expressed as N-terminal GST fusion protein with a C-terminal noncleavable hexahistidine tag. Affinity-purified ERK2 was cleaved by the tobacco etch virus (TEV) protease

and samples were further purified by ion exchange on a Resource Q column (GE Healthcare). Double affinity purified RSK1 was also cleaved by the TEV protease and the sample was further purified on a HiTrap Blue-Sepharose column (GE Healthcare). Purified kinases were mixed in 1:1.2 ratio with ERK2 in excess and the sample was gel filtrated on a Superdex 75 column (GE Healthcare). Fractions corresponding to the stoichiometric complex were pooled and the sample was concentrated to 10 mg/mL.

Crystallization, Structure Solution, and Refinement. The stock solution of the final protein sample was supplemented with 2 mM adenosine 5′-(β,γ-imido)triphosphate (AMPPNP) and 2 mM $MgCl_2$. Crystallization was done in standard sitting drop vapor-diffusion set-up at 23 °C. The crystallization solution consisted of 0.1 M Mes pH = 6.25, 15% (vol/vol) PEG4000, 0.125 M $(NH_4)_2SO_4$ and 2% (wt/vol) benzamidine. Drops with plate-shaped crystals (with an average size of 0.15 mm × 0.15 mm × 0.02 mm) were supplemented with 10% (vol/vol) glycerol before flash cooling in liquid nitrogen. Data were collected on the PXIII beam line of the Swiss Light Source (Villigen) at 100 K. Details on data collection, analysis, and structure determination are given in *SI Appendix, Methods*.

MD Simulations. Starting MD models for ERK2–RSK1 and ppERK2–RSK1 were generated from the ERK2–RSK1 crystallographic complex. The crystal structure of double-phosphorylated ERK2 (ppERK2; PDB ID: 2ERK) was superimposed with ERK2 from the unphosphorylated ERK2–RSK1 crystal structure (giving the starting model for ppERK2–RSK1). The phosphate groups on Thr185 and Tyr187 were removed from the ppERK2–RSK1 model (giving the starting model for the unphosphorylated ERK2–RSK1 complex). In all calculations, the GROMACS ver. 4.5.5 program package (37), the Amber-03 (38) force field was applied along with neutralizing Na^+ counter ions and numerous TIP3P (39) explicit water molecules filling a 5-Å spacing between the protein parts and the edges of the cubic simulation box. The lengths of the unrestrained MD runs were 1 μs (ppERK2–RSK1) or 150 ns (ERK2–RSK1). Further details on MD simulation parameters and processing of MD results are given in *SI Appendix, Methods*.

ERK2→RSK1 Activation Assays. For in vitro assays, recombinant-expressed and purified proteins were used, and RSK1 phosphorylation was monitored by P32 autoradiography or by phospho-Thr573(RSK1) Western blots. Further details on in vitro kinase assays are given in *SI Appendix, Methods*. For cell-based assays, RSK1 constructs were subcloned into modified pcDNA 3.1 vectors with N-terminal Venus fluorescent protein and C-terminal FLAG fusion tags (Invitrogen). HEK293T cells were cultured in 96-well plates as described in detail in *SI Appendix, Methods*. Cells were transfected with 0.4 μg RSK1 DNA constructs and were serum starved for 24 h. The media was removed after 40 h from DNA transfection and 100 μL PBS was added to wells. ERK pathway stimulation was started by addition of EGF (Sigma, E9644) in 100 ng/mL concentration to each well and stimulation was terminated at different time points by adding 35 μL of 4× SDS loading buffer to wells. Cells were lysed and 10 μL of each sample was subjected to SDS/PAGE. Western blots for monitoring RSK1 phosphorylation on Thr573 were done using the phospho-p90RSK (Thr573) primary antibody (Cell Signaling, 9346). The phospho-p44/42 MAPK (Erk1/2) (Thr202/Tyr204) antibody (Cell Signaling, 9101) and an anti-FLAG antibody (Sigma, F1804) were used to check endogenous ppERK2 and heterologous RSK1 protein levels, respectively.

ACKNOWLEDGMENTS. We thank József Kardos and Éva Bulyáki for their help in CD measurements, András Patthy for excellent peptide synthesis, PRACE for awarding us access to resources Monte Rosa based in Switzerland at CSCS Swiss National Supercomputing Centre, and NIIFI SC based in Hungary at NIIF National Information Infrastructure Development Institute. A.R. is supported by the "Lendület" grants from the Hungarian Academy of Sciences (LP2013-57) and by an International Senior Research fellowship from the Wellcome Trust. The work was also supported by OTKA NK101072 (to A.B.) and a MedinProt grant (to A.R. and C.H.).

1. Taylor SS, Kornev AP (2011) Protein kinases: Evolution of dynamic regulatory proteins. *Trends Biochem Sci* 36(2):65–77.
2. Endicott JA, Noble MEM, Johnson LN (2012) The structural basis for control of eukaryotic protein kinases. *Annu Rev Biochem* 81:587–613.
3. Johnson GL, Lapadat R (2002) Mitogen-activated protein kinase pathways mediated by ERK, JNK, and p38 protein kinases. *Science* 298(5600):1911–1912.
4. Raman M, Chen W, Cobb MH (2007) Differential regulation and properties of MAPKs. *Oncogene* 26(22):3100–3112.
5. Canagarajah BJ, Khokhlatchev A, Cobb MH, Goldsmith EJ (1997) Activation mechanism of the MAP kinase ERK2 by dual phosphorylation. *Cell* 90(5):859–869.
6. Pearce LR, Komander D, Alessi DR (2010) The nuts and bolts of AGC protein kinases. *Nat Rev Mol Cell Biol* 11(1):9–22.
7. Cargnello M, Roux PP (2011) Activation and function of the MAPKs and their substrates, the MAPK-activated protein kinases. *Microbiol Mol Biol Rev* 75(1):50–83.
8. Gavin AC, Nebreda AR (1999) A MAP kinase docking site is required for phosphorylation and activation of p90(rsk)/MAPKAP kinase-1. *Curr Biol* 9(5):281–284.
9. Tanoue T, Maeda R, Adachi M, Nishida E (2001) Identification of a docking groove on ERK and p38 MAP kinases that regulates the specificity of docking interactions. *EMBO J* 20(3):466–479.
10. Smith JA, et al. (2000) Creation of a stress-activated p90 ribosomal S6 kinase. The carboxyl-terminal tail of the MAPK-activated protein kinases dictates the signal transduction pathway in which they function. *J Biol Chem* 275(41):31588–31593.
11. Garai Á, et al. (2012) Specificity of linear motifs that bind to a common mitogen-activated protein kinase docking groove. *Sci Signal* 5(245):ra74.
12. Dalby KN, Morrice N, Caudwell FB, Avruch J, Cohen P (1998) Identification of regulatory phosphorylation sites in mitogen-activated protein kinase (MAPK)-activated protein kinase-1a/p90rsk that are inducible by MAPK. *J Biol Chem* 273(3):1496–1505.
13. Ben-Levy R, et al. (1995) Identification of novel phosphorylation sites required for activation of MAPKAP kinase-2. *EMBO J* 14(23):5920–5930.
14. Soundararajan M, et al. (2013) Structures of Down syndrome kinases, DYRKs, reveal mechanisms of kinase activation and substrate recognition. *Structure* 21(6):986–996.
15. Kornev AP, Taylor SS, Ten Eyck LF (2008) A helix scaffold for the assembly of active protein kinases. *Proc Natl Acad Sci USA* 105(38):14377–14382.
16. Rellos P, et al. (2010) Structure of the CaMKIIdelta/calmodulin complex reveals the molecular mechanism of CaMKII kinase activation. *PLoS Biol* 8(7):e1000426.
17. Malakhova M, et al. (2008) Structural basis for activation of the autoinhibitory C-terminal kinase domain of p90 RSK2. *Nat Struct Mol Biol* 15(1):112–113.
18. Underwood KW, et al. (2003) Catalytically active MAP KAP kinase 2 structures in complex with staurosporine and ADP reveal differences with the autoinhibited enzyme. *Structure* 11(6):627–636.
19. ter Haar E, Prabhakar P, Liu X, Lepre C (2007) Crystal structure of the p38 alpha-MAPKAP kinase 2 heterodimer. *J Biol Chem* 282(13):9733–9739.
20. Meng W, et al. (2002) Structure of mitogen-activated protein kinase-activated protein (MAPKAP) kinase 2 suggests a bifunctional switch that couples kinase activation with nuclear export. *J Biol Chem* 277(40):37401–37405.
21. Stokoe D, et al. (1992) MAPKAP kinase-2; a novel protein kinase activated by mitogen-activated protein kinase. *EMBO J* 11(11):3985–3994.
22. Good MC, Zalatan JG, Lim WA (2011) Scaffold proteins: Hubs for controlling the flow of cellular information. *Science* 332(6030):680–686.
23. Rainey MA, Callaway K, Barnes R, Wilson B, Dalby KN (2005) Proximity-induced catalysis by the protein kinase ERK2. *J Am Chem Soc* 127(30):10494–10495.
24. Lee S, et al. (2011) A model of a MAPK•substrate complex in an active conformation: A computational and experimental approach. *PLoS ONE* 6(4):e18594.
25. Pontius BW (1993) Close encounters: why unstructured, polymeric domains can increase rates of specific macromolecular association. *Trends Biochem Sci* 18(5):181–186.
26. Dunker AK, et al. (2001) Intrinsically disordered protein. *J Mol Graph Model* 19(1):26–59.
27. White A, Pargellis CA, Studts JM, Werneburg BG, Farmer BT, 2nd (2007) Molecular basis of MAPK-activated protein kinase 2:p38 assembly. *Proc Natl Acad Sci USA* 104(15):6353–6358.
28. Malecka KA, Peterson JR (2011) Face-to-face, pak-to-pak. *Structure* 19(12):1723–1724.
29. Oliver AW, Knapp S, Pearl LH (2007) Activation segment exchange: A common mechanism of kinase autophosphorylation? *Trends Biochem Sci* 32(8):351–356.
30. Wang J, Wu JW, Wang ZX (2011) Structural insights into the autoactivation mechanism of p21-activated protein kinase. *Structure* 19(12):1752–1761.
31. Mieczkowski C, Iavarone AT, Alber T (2008) Auto-activation mechanism of the Mycobacterium tuberculosis PknB receptor Ser/Thr kinase. *EMBO J* 27(23):3186–3197.
32. Nayak V, et al. (2006) Structure and dimerization of the kinase domain from yeast Snf1, a member of the Snf1/AMPK protein family. *Structure* 14(3):477–485.
33. Brennan DF, et al. (2011) A Raf-induced allosteric transition of KSR stimulates phosphorylation of MEK. *Nature* 472(7343):366–369.
34. Xie T, et al. (2013) Structural insights into RIP3-mediated necroptotic signaling. *Cell Reports* 5(1):70–78.
35. Cai Z, Chehab NH, Pavletich NP (2009) Structure and activation mechanism of the CHK2 DNA damage checkpoint kinase. *Mol Cell* 35(6):818–829.
36. Bardwell AJ, Frankson E, Bardwell L (2009) Selectivity of docking sites in MAPK kinases. *J Biol Chem* 284(19):13165–13173.
37. Pronk S, et al. (2013) GROMACS 4.5: A high-throughput and highly parallel open source molecular simulation toolkit. *Bioinformatics* 29(7):845–854.
38. Duan Y, et al. (2003) A point-charge force field for molecular mechanics simulations of proteins based on condensed-phase quantum mechanical calculations. *J Comput Chem* 24(16):1999–2012.
39. Jorgensen WL, Chandrasekhar J, Madura JD, Impey RW, Klein ML (1983) Comparison of simple potential functions for simulating liquid water. *J Chem Phys* 79:926.